Available online at www.sciencedirect.com

SciVerse ScienceDirect

journal homepage: www.JournalofSurgicalResearch.com

Association for Academic Surgery

BMPR1A mutations in juvenile polyposis affect cellular localization

James R. Howe,[1] Fadi S. Dahdaleh, MD,[1] Jennifer C. Carr, MD, Donghong Wang, MS, Scott K. Sherman, MD, and James R. Howe, MD*

Division of Surgical Oncology and Endocrine Surgery, Department of Surgery, University of Iowa Hospitals and Clinics, Iowa City, Iowa

ARTICLE INFO

Article history:
Received 27 August 2012
Received in revised form
19 November 2012
Accepted 10 January 2013
Available online 1 February 2013

Keywords:
Bone morphogenetic protein
Juvenile polyposis
Missense

ABSTRACT

Background: Juvenile polyposis (JP) is characterized by the development of hamartomatous polyps of the gastrointestinal tract that collectively carry a significant risk of malignant transformation. Mutations in the bone morphogenetic protein receptor type 1A (BMPR1A) are known to predispose to JP. We set out to study the effect of such missense mutations on BMPR1A cellular localization.

Methods: We chose eight distinct mutations for analysis. We tagged a BMPR1A wild-type (WT) expression plasmid with green fluorescent protein on its C-terminus. Site-directed mutagenesis was used to recreate JP patient mutations from the WT–green fluorescent protein BMPR1A plasmid. We verified mutant expression vector sequences by direct sequencing. First, we transfected BMPR1A expression vectors into HEK-293T cells; then, we performed confocal microscopy to determine cellular localization. Four independent observers used a scoring system from 1 to 3 to categorize the degree of membrane *versus* cellular localization.

Results: Of the eight selected mutations, one was within the signaling peptide, four were within the extracellular domain, and three were within the intracellular domain. The WT BMPR1A vector had strong membrane staining, whereas all eight mutations had much less membrane and much more intracellular localization. Enzyme-linked immunosorbent assays for BMPR1A demonstrated no significant differences in protein quantities between constructs, except for one affecting the start codon.

Conclusions: Bone morphogenetic protein receptor type 1A missense mutations occurring in patients with JP affected cellular localization in an *in vitro* model. These findings suggest a mechanism by which such mutations can lead to disease by altering downstream signaling through the bone morphogenetic protein pathway.

1. Introduction

Juvenile polyposis (JP) is a rare syndrome affecting between one person per 16,000 and one per 100,000 [1]. The disease is characterized by the predisposition to hamartomatous polyps generally found in the colorectum, but may also involve the upper gastrointestinal tract, predominantly the stomach. It is inherited in an autosomal dominant fashion, and those with JP have a 39% chance of developing colorectal cancer over their lifetime [2].

* *Corresponding author.* Division of Surgical Oncology and Endocrine Surgery, Department of Surgery, University of Iowa Hospitals and Clinics, 200 Hawkins Drive, Iowa City, IA 52242-1086. Tel.: +1 319 356 1727; fax: +1 319 356 1218.
E-mail address: james-howe@uiowa.edu (J.R. Howe).

[1] Drs. Howe and Dahdaleh share first authorship of this article.

0022-4804/$ – see front matter © 2013 Elsevier Inc. All rights reserved.
http://dx.doi.org/10.1016/j.jss.2013.01.015

Germline mutations in two genes are known to cause JP: *SMAD4* [3], the common intracellular mediator of the transforming growth factor-β pathway, and bone morphogenetic protein receptor 1A (BMPR1A) [4]. Approximately 20%–25% of JP cases result from mutations or deletions of BMPR1A, and 20%–25% from *SMAD4* [5]. The genetic origin of the other half of JP cases is currently unknown.

The bone morphogenetic protein (BMP) signaling pathway influences many cell processes, including cell growth, differentiation, and apoptosis [6]. The BMP type 1 receptor is a transmembrane cell-surface receptor that forms a complex with the type 2 receptor (BMPR2), which binds to BMP ligands (BMP2, 4, and 7). After this occurs, BMPR1A phosphorylates receptor-regulated SMADs (R-SMADs, of which SMAD1, 5, and 8 are specific for the BMP pathway); then these bind to SMAD4 and this complex enters the nucleus. The R-SMAD/SMAD4 complex then binds to DNA and regulates transcription, in conjunction with other nuclear DNA-binding proteins (Fig. 1). It is intuitive that nonsense mutations will have significant effects on protein function, by virtue of truncation and loss of important domains, as well as increased degradation. However, the effect of missense mutations is not always as obvious. The substitution of one amino acid for another may cause changes in a protein's three-dimensional conformation, which may affect its interactions with other proteins, but these alterations can also be of minimal functional significance. The objective of this study was to examine the effects of different BMPR1A missense mutations found in JP patients on the cellular localization of this protein.

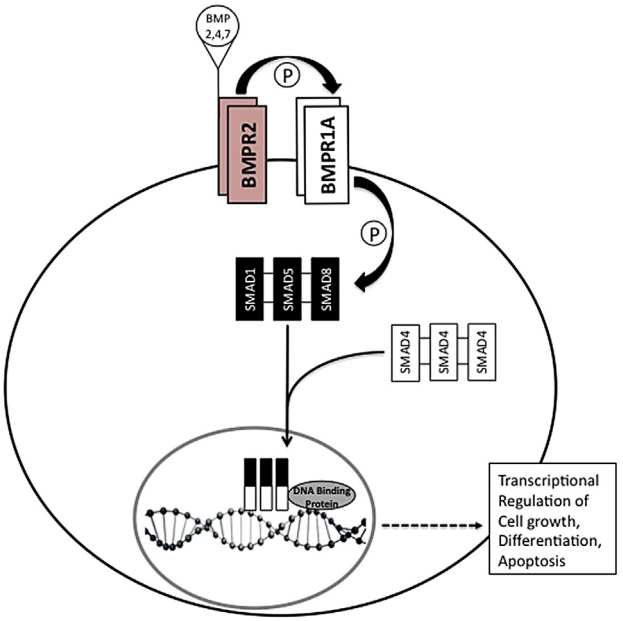

Fig. 1 – Overview of BMP-signaling pathway. The BMPR2 dimers at the cell membrane bind BMP 2, 4, or 7, facilitated by their binding to dimers of BMPR1A. Upon ligand binding, BMPR2 phosphorylates BMPR1A, which then phosphorylates intracellular SMAD1, 5, and/or 8. Oligomers of SMAD1, 5, or 8 then associate with oligomers of SMAD4, migrate into the nucleus, and associate with DNA-binding proteins. This complex binds directly to DNA to regulate transcription of genes involved in cell growth, differentiation, and apoptosis.

2. Materials and methods

2.1. *Identification of BMPR1A mutations*

We collected JP patient blood samples under a protocol approved by the Institutional Review Board at the University of Iowa. We extracted genomic DNA from peripheral blood by salting out [7] or using the Puregene DNA purification kit (Gentra Systems, Minneapolis, MN), and from lymphoblastoid cell lines by the Qiagen AllPrep DNA mini kit (Qiagen, Valencia, CA). We amplified DNA by polymerase chain reaction (PCR) using primers that flanked all 11 coding exons of BMPR1A. We purified PCR products using the QIAquick Gel Extraction Kit (Qiagen). Then, we sequenced PCR products by dideoxy cycle sequencing followed by electrophoresis through an ABI model 3730 automated sequencer (Applied Biosystems, Foster City, CA). Sequences were screened in Sequencher (Gene Codes, Ann Arbor, MI), and coding or splice site mutations of BMPR1A identified. We selected eight distinct missense mutants for use in transfection experiments.

2.2. *Site-directed mutagenesis*

We obtained a green fluorescent protein (GFP) tagged wild-type BMPR1A expression vector in a pCMV6-AC-GFP construct (Origene, Rockville, MD). We used a PCR-based, site-directed mutagenesis approach to generate individual mutations. Primers containing specific patient mutations were designed using the QC Primer Design Software (Stratagene-Agilent, Santa Clara, CA). We then used *Pfu*Ultra (Stratagene-Agilent) to amplify mutant constructs by PCR under the following conditions: 95°C for 30 s, 65°C for 1 min, and then 7 min at 68°C for 18 cycles. We then used resulting plasmids to transform XL1-Blue competent bacterial cells, and selected colonies and extracted DNA using the PureLink Plasmid Quick Miniprep Kit (Life Technologies, Carlsbad, CA). All plasmids were then sequenced to verify the presence of the desired mutations.

2.3. *Transfection of cells*

We used human embryonic kidney cells containing the SV40 large T-antigen (HEK-293T) for transfection experiments because of their ease and reliability. These were obtained from the American Type Culture Collection (ATCC, Manassas, VA). We plated groups of cells onto glass coverslips in different wells of multiple six-well plates. Cells were cultured in Dulbecco's modified Eagle's medium (DMEM; Life Technologies) containing 10% fetal bovine serum (FBS) and 1% penicillin G-streptomycin sulfate to ~50%–80% confluence before transfection. Transfection was optimized by testing under six different conditions to maximize expression of GFP-tagged BMPR1A (Table 1). We transfected 1–2 μg of each pCMV6-AC-GFP construct in a 1:3 ratio with Lipofectamine 2000 (Life Technologies) into these cells. The cells were then starved by the addition of DMEM without FBS for 4 h after transfection.

Table 1 – Different conditions used for transfection.

Trial number	Time until viewing (h)	% Confluence	BMP4 added	Amount of DNA (μg)
1	48	80	Yes	1
2	48	80	Yes	2
3	48	80	No	2
4	48	50	Yes	2
5	24	80	Yes	2
6	24	80	No	2

At the end of the 4 h, we resuspended the cells in DMEM/FBS and added 25 μg BMP4 ligand to stimulate expression.

2.4. *Confocal microscopy and scoring*

After incubation for 24–48 h before confocal microscopy, we removed the media and fixed cells in 10% formalin. We removed the coverslips from the six-well plates and placed them on microscope slides. A DAPI stain (Life Technologies) was applied to the cells and incubated at room temperature for 10 min to make the nuclei visible under confocal microscopy. We then viewed specimens under ×20 and ×63 magnification on a BioRad Radiance 2100 confocal microscope (BioRad Laboratories, Hercules, CA). The images were captured and contrast-adjusted with ImageJ (http://rsbweb.nih.gov/ij/). Four independent observers who were blinded to construct identity reviewed the images. After assessing all cells, each image was given a score ranging from 1 to 3, with 3 indicating predominantly intracellular localization of GFP-tagged BMPR1A, 2 showing both intracellular and membrane staining, and 1 predominant staining of the cell membrane. We then calculated the mean scores for each image.

2.5. *Protein extraction and enzyme-linked immunosorbent assay*

We grew HEK293T cells to confluence in six-well plates, transfected as above with the indicated constructs; for enzyme-linked immunosorbent assay (ELISA) experiments, we co-transfected the cells with a β-galactosidase plasmid to allow for correction of transfection efficiency. After 24–48 h, we lysed cells with 2× RIPA buffer with complete mini protease inhibitor cocktail tablets (Roche Diagnostics GmbH, Manheim, Germany). Samples were then vortexed, sonicated, and quantified using the Pierce BCA protein assay kit (Thermo Scientific, Waltham, MA) and Infinite M200 microplate-reader (Tecan, Durham, NC). We diluted 15 μg protein in 6 mol/L sodium iodide to a volume of 50 μL; this amount was distributed into each well of 96-well plates and incubated at 4°C overnight. Each well was washed twice with 200 μL/well washing buffer (1 × phosphate-buffered saline (PBS)–Tween 20 [0.05% Tween 20]) and then each well was incubated with 1% bovine serum albumin (BSA) in PBS at room temperature for 2 h to block nonspecific binding. We added 50 μL BMPR1A primary monoclonal antibody (catalog number MAB2406; R&D Systems, Minneapolis, MN) diluted in a 1:500 ratio with 1% BSA in PBS to each well of BMPR1A plates, and 50 μL β-galactosidase antibody (catalog number sc-40; Santa Cruz Biotechnology) to duplicate plates. Plates were left at room temperature for 2 h and washed twice more with the above buffer; then 50 μL horseradish peroxidase–conjugated goat anti-mouse antibody (catalog number C2011; Santa Cruz Biotechnology, Santa Cruz, CA; diluted in a 1:250 ratio with 1% BSA in PBS) was added to each well in the plate and incubated at room temperature for 1 h. We washed the plate three times with washing buffer, then added 50 μL 3,3′,5,5′-tetramethylbensidine (Invitrogen-Life Technologies, Grand Island, NY) to each well and incubated the plate in the dark for 10 min. We finally added 50 μL 2 mol/L H_2SO_4 to stop coloration and measured relative protein levels using the microplate reader set at 450 nm. Optical density values obtained for the different BMPR1A constructs were then normalized using the results obtained with β-galactosidase for each experiment relative to those obtained from the wild-type vector, then expressed as a percentage of BMPR1A relative to the wild-type vector.

2.6. *BRE-Luc experiments*

We cultured HEK-293T cells in DMEM containing 10% FBS and 1% penicillin G-streptomycin sulfate. After growth to 90% confluence, the cells were co-transfected with 1 μg of the BRE-Luc vector (a plasmid reporter vector with a BMP-responsive element promoter cloned upstream from a luciferase gene) [8], 1 μg of a BMPR1A expression vector (wild type or mutants), and 200 ng of *Renilla* (internal control vector for transfection efficiency), using 6 μL Lipofectamine 2000 reagent (Invitrogen). Each transfection was performed in triplicate. After 4 h, we added fresh media. At 48 h post-transfection, we added 500 μL lysis buffer to the cells, which we incubated at room temperature for 15 min. We transferred 20 μL lysate to a reading tube that contained 100 μL Luciferase Assay Reagent II (Promega, Madison, WI) solution, and measured luciferase activity at 562 nm for 10 s using a TD 20/20 luminometer (Turner BioSystems, Sunnyvale, CA). Once initial readings were performed, 100 μL Stop and Glo reagent (Promega) was added, and *Renilla* luciferase activity was measured at 480 nm for 10 s. We determined the final amount of luciferase activity for each construct by subtracting the background luciferase activity of the control pGL3 basic vector without construct, and then normalizing it to *Renilla* luciferase activity for each individual reaction. We then performed a Student *t*-test to assess the statistical significance of differences between triplicate results obtained for each mutant construct relative to the wild type.

2.7. In silico *evaluation of mutations*

We assessed each BMPR1A missense mutation used for deleterious effect using the Web-based ANNOVAR pipeline [9]. This included the algorithms SIFT [10], LRT [11], Blosum62 [12], Polyphen2 [13], MutationTaster [14], GERP++ [15], and PhyloP [16].

3. Results

3.1. *Determination of optimal transfection conditions*

To determine optimal conditions for transfection and subsequent viewing by confocal microscopy, we altered four

distinct variables (time, confluence, DNA concentration, and presence of BMP4) in 12 separate colonies of cells: six were wild-type and the other six were mutant. We exposed both the mutant and wild-type colonies to the same six conditions. Of these experimental conditions, transfection of 2 μg at 50% confluence, followed by incubation for 48 h in the presence of BMP4, resulted in the highest expression of GFP and clearest pictures with confocal microscopy. We used these conditions for all subsequent transfections.

3.2. Results of ELISA and Bre-Luc assays

The total level of BMPR1A protein by ELISA was similar among all of the constructs and wild-type levels, with the exception of 1A > C (M1L) (Table 2). The latter mutation affects the initiation codon for translation, possibly leading to loss of antibody binding. For the other mutations, the greatest changes in BMPR1A were only 32.4% and 26.9% more or less than the wild type, respectively. The mean of these seven mutant protein levels was 101.6% of wild-type levels (range, 73%–132%; standard deviation [SD], 18.5%). This suggests that the lack of membrane staining with all but one of the mutant constructs likely did not result from reduced levels of protein.

To understand the function of these mutant proteins, we evaluated changes in BMP signaling, as measured by the BMP-specific reported Bre-Luc. These were much more variable: The mean of all mutant samples was 77.4% that of wild type, with an SD of 44.8%. Five of eight constructs had reduced BMP signaling activity, ranging as low as 4.6% for the 1013C > A mutation to 72.8% for the 184T > G change (Table 2). The 170C > G and 761G > A were higher than wild type (123% and 146%, respectively); interestingly, the 1A > C alteration was essentially the same as wild type, even though the protein level was absent by ELISA. There was no clear correlation between the localization score and BMP signaling, although both mutations scoring a mean of 3 had low signaling. Conversely, of the two mutations with a mean score of 2, one had reduced signaling, whereas the other was increased. These results suggest that different specific mutations exert varied effects on BMPR1A signaling activity, as measured by this surrogate plasmid vector.

Table 2 – Results of scoring by observers blinded to protocol, and amount of protein detected by ELISA and BMP signaling relative to wild type.

Genotype	Localization score	ELISA (% of WT)	BMP signaling (% of WT)
WT	1	100.6	100
1A > C	2.25	0.0	102.8
170C > G	2	96.6	123.1*
184T > G	2.75	88.8	72.8*
233C > T	3	132.4	44.6*
245 G > A	2	120.9	36.8*
761 G > A	2.25	106.0	146.0
1013C > A	3	73.1	4.6*
1327C > T	2.75	93.6	88.2

*Significantly different from wild type (WT).

3.3. Patterns of membrane staining

With evidence that mutant proteins are expressed but have different signaling activity, we next investigated whether abnormal localization of mutant transcripts occurs. All eight missense constructs as well as wild-type were tagged with the sequence for GFP and transfected into HEK-293T cells. Confocal microscopy revealed the location of the expressed protein. In general, approximately 20% of cells had visible expression of GFP-tagged BMPR1A. The wild-type construct showed strong staining at the membrane with only minimal intracellular protein (Fig. 2). None of the mutant constructs showed this degree of cell membrane staining with GFP. Some, such as 245 G > A (Fig. 3) and 170C > G, had faint membrane staining but markedly more intracellular fluorescence than wild-type cells. Others, such as 1013C > A (Fig. 4) and 233C > T, showed near-complete intracellular localization. With high-power microscopy, we observed these mutant proteins around the nucleus, with little or no visible membrane fluorescence.

To quantify protein localization, four observers scored confocal images from 1 to 3, with 1 indicating localization at the membrane and 3 indicating localization solely within the cell. All observers unanimously scored the wild-type protein as 1, whereas all missense constructs were scored as intracellular, ranging between 2 and 3 (Table 2). Taken together, these results show that although wild-type BMPR1A is observed almost exclusively at the membrane of BMP-stimulated cells, JP-associated mutant BMPR1A receptors show varying degrees of mislocalization to the intracellular compartment. Furthermore, the 1013C > A and 233C > T mutations, which showed the lowest levels of membrane-localized protein, also demonstrated the lowest BMP pathway signaling by Bre-Luc reporter, which suggests that mislocalization can be associated with impaired protein function.

3.4. In silico mutation analysis

To investigate the relationship between our observations and *in silico* predictions of altered protein function, we analyzed all mutations with several pathogenicity prediction tools for missense mutations (Table 3). As expected for known disease variants, all were predicted to be deleterious by at least five of seven tools. The 184T > G, 245 G > A, and 1327C > T mutations were scored as deleterious by all seven tools, and only two mutations, 1A > C by BLOSUM and PolyPhen2 and 170C > G by PolyPhen2, were predicted to be tolerated by any algorithm. Strong predictions of pathogenicity were assigned to all mutations by GERP++, Mutation Taster, LRT, and PhyloP, which reflects high conservation of the affected residues among homologous proteins. Variations among different mutations' pathogenicity scores did not correlate with observed differences in receptor localization or BMP signaling.

4. Discussion

This study demonstrates that BMPR1A missense mutations, as found in the germline of JP patients, did not result in decreased protein levels *in vitro* (except one affecting the

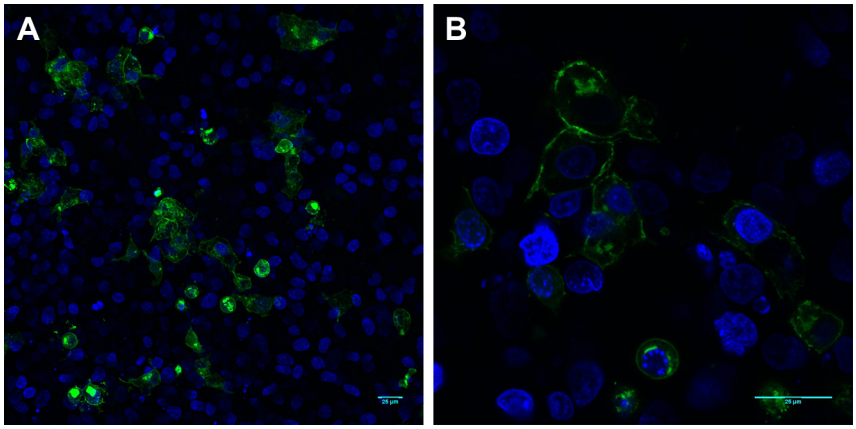

Fig. 2 – Predominant membrane staining pattern (score of 1) in HEK-293T cells transfected with wild-type BMPR1A. The nuclei are blue and BMPR1A protein appears as green. (A) Low-power view (×20 magnification). (B) High-power view (×63 magnification).

initiation codon), and five of eight led to reduced BMP signaling, as measured by a BMP-specific reporter vector. More strikingly, all of the GFP-tagged proteins resulting from these mutant expression vector constructs showed reduced localization to the cell membrane, with accumulation in the cytoplasm. This shows a direct, functional consequence of these mutations, and one explanation for impairment of the BMP pathway in these patients. Determining the specific mechanisms by which these point mutations lead to impaired trafficking to the cell membrane will require further study, but several insights become evident from previous studies.

Beginning with different predictive algorithms for missense mutations, all appeared to be potentially damaging using most of these programs (Table 3). The two exceptions were the mutation in the signal peptide (1A > C; M1L) and in the extracellular domain (170C > G; P57R). The N-terminal region of BMPR1A contains a signal peptide (amino acids 1–23), which presumably helps direct localization and transport of the protein. Therefore, it is not surprising that 1A > C (M1L) mutation might lead to reduced membrane-bound receptor. The results for this mutation in this study were conflicting: We found no protein by ELISA, whereas BMP-signaling was comparable to wild type, and GFP expression was readily observed and predominantly cytoplasmic. A missense mutation affecting the initiation codon would be expected to be faithfully copied into mRNA; then, at the 40S ribosomal level it would not be recognized. Scanning in a 3′ direction would continue until another AUG was found in the appropriate context to begin translation into protein. The next AUG triplet in the BMPR1A mRNA occurs in exon 2, at position 85 of the wild-type sequence, which also has a purine 3 bases upstream, which increases the chance of recognition of this start site [17]. If translation began here, it would remain in-frame but result in loss of the first 28 amino acids, while preserving the remainder of the protein. Details on the specific epitope recognized by the BMPR1A monoclonal antibody used in this study are lacking, but it was raised using an immunogen consisting of amino acids 1–152 (R&D Systems, personal communication). Our results suggest that the antibody likely binds within these first 28 amino acids, and therefore no protein was detected by ELISA. However, its GFP-tag was seen by confocal microscopy, and it could still drive BMP signaling by virtue of preserving most of the protein.

The extracellular domain of BMPR1A (residues 24–152) is the site of BMP-ligand binding, and the three other extracellular domain mutations (Y62D, T78I, and C82Y) were all

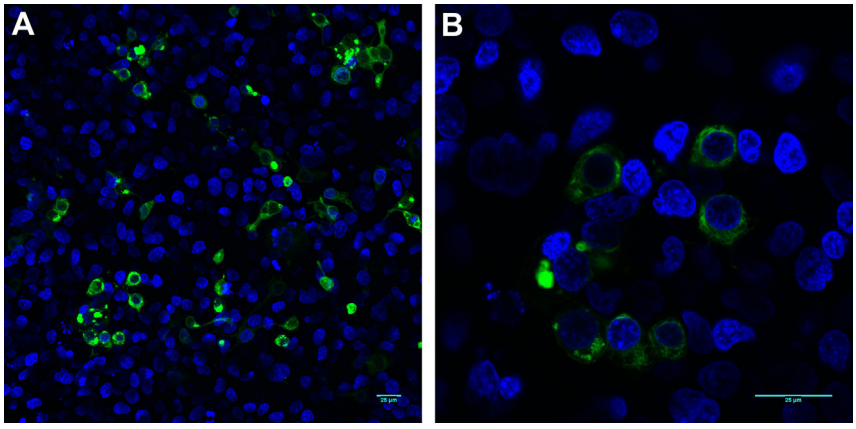

Fig. 3 – Score of 2 (mutation 245 G > A). Most of GFP-tagged BMPR1A is intracellular; a minority localizes to the cell membrane. (A) Low-power view (×20 magnification). (B) High-power view (×63 magnification).

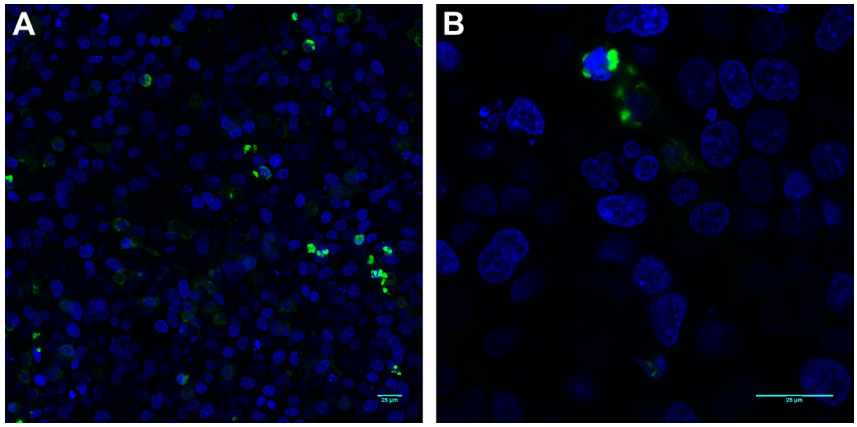

Fig. 4 – Score of 3 (mutation 1013C > A). Almost all GFP-tagged BMPR1A localizes intracellularly and close to the nucleus, with almost no GFP staining visible along the cell membranes. (A) Low-power view (×20 magnification). (B) High-power view (×63 magnification).

predicted to be deleterious using each algorithm. These occurred in the cysteine-rich portion involving residues 61–130, where there are five disulfide bonds (between amino acids 61 and 82, 63 and 67, 76 and 100, 110 and 124, and 125–130; www.nextprot.org/db/entry/NX_P36894/sequence). The C82Y mutation directly alters one of these cysteine residues, and it is likely that the others would also interfere with the protein's normal three-dimensional configuration, which might be needed to form other disulfide bonds important for BMP ligand binding. The Y62D mutation would change a hydrophobic tyrosine to a negatively charged aspartate, and the interaction between BMP-2 with BMPR1A requires a hydrophobic pocket consisting of Y62, P60, and Y99 residues [18]. The T78I mutation would change a polar, uncharged threonine to a hydrophobic isoleucine, which might also alter BMP binding if it were to get to the membrane. Kotzsch *et al.* [19] have also shown that three extracellular domain mutations found in JP patients (P34R, Y39D, and T55I) that are not main determinants for binding to BMP ligands or within the core hydrophobic regions, also inactivate BMP-2 signaling [19]. They found that these mutant proteins lost their folding ability relative to wild-type protein, but they appeared to migrate normally from cytoplasm to the cell membrane, which is in contrast to what was found with extracellular domain mutations here.

A few studies have further examined this phenomenon in BMPR1A's ligand binding partner, the BMPR2 receptor, using HeLa cells transfected with GFP-tagged mutant expression vectors. Radarakanchana *et al.* [20] showed that four mutants affecting cysteines in the ligand binding domain and two in the kinase domain failed to reach the cell surface and accumulated in the endoplasmic reticulum (ER), whereas those affecting aspartate or arginine made it to the membrane [20]. Sobelewski *et al.* [21] performed similar experiments using the C118W mutant from the cysteine-rich, ligand-binding domain of BMPR2. The mutant BMPR2 was again retained in the ER, whereas the wild-type protein demonstrated predominantly membrane staining (as seen with BMPR1A in this study). Interestingly, they found that mutant BMPR2 colocalized and was retained with BMP type 1 receptors in the cytoplasm, whereas wild-type receptors did the same at the cell membrane. The authors also showed that surface expression of mutant BMPR2 could be restored by treating cells with the chemicals chaperones thapsigargin, glycerol, or 4-PBA, and that the mutant protein restored BMP signaling. They pointed out that accumulation of mutant proteins within the ER may occur through abnormal processing, changes in degradation, or altered ER stress response, and that this is common in various disease states.

Table 3 – Results of *in silico* predictions of mutation effect on protein function.

Nucleotide change; amino acid change	PhyloP	BLOSUM 62	SIFT	Poly Phen2	LRT	Mutation Taster	GERP++
1A > C; M1L	1.00	2.00	1.00	0.01	1.00	1.00	5.14
170C > G; P57R	1.00	−2.00	0.14	0.00	1.00	0.97	5.66
184T > G; Y62D	1.00	−3.00	0.97	0.99	1.00	1.00	4.50
233C > T; T78I	1.00	−1.00	1.00	0.82	1.00	1.00	5.48
245 G > A; C82Y	1.00	−2.00	1.00	1.00	1.00	1.00	5.48
761G > A; R254H	1.00	0.00	1.00	0.79	1.00	1.00	5.49
1013C > A; A338D	1.00	−2.00	0.93	0.77	1.00	1.00	4.81
1327C > T; R443C	1.00	−3.00	1.00	1.00	1.00	1.00	5.58

For PhyloP, SIFT, PolyPhen2, LRT, and Mutation Taster, range is 0–1, with >0.95 likely deleterious, <0.05 likely benign. For BLOSUM62, range is −3 to +3, with <0 likely deleterious. For GERP++, values >0 indicate likely constrained residue.

In this study, there did not appear to be a direct correlation between the domain of the mutation and the degree of abnormal localization of BMPR1A protein. No mutations studied involved the transmembrane domain (amino acids 153–176), and to date, no germline mutations have been reported in this region of the gene in JP patients (although one SNP, I164V, has been reported from the 1000 genomes project, and an M167I mutation has been found in a lung cancer sample).

The remaining mutations we examined were in the intracellular domain (amino acids 177–532), which contains the GS region (serine-glycine repeats where BMPR1A is phosphorylated by type 2 receptors, residues 204-233), and the kinase domain (where SMAD proteins bind and are phosphorylated, residues 234–525). These mutations included R254H, A338D, and R443C, which were all within the kinase domain and predicted to be deleterious by each algorithm (Table 3). Sobolewski *et al.* [21] observed that a BMPR2 mutant in the intracellular cysteine kinase domain (C483R) was retained in the cytoplasm, and cell membrane localization could be achieved by treatment with the chemical chaperone 4-PBA [21].

Two groups discovered that the splicing factor 3b subunit 4, a nuclear protein, interacts with the intracellular domain of BMPR1A by yeast two-hybrid assays [22,23]. Nishanian and Waldman [22] showed that the GS domain was important for BMPR1A's interaction with the protein, and that deletion mutants of the kinase domain could mask this association. Watanabe *et al.* [23] found that as splicing factor 3b subunit 4 expression increased, cell membrane localization of BMPR1A decreased, providing an example of decreased trafficking as a result of interaction with other intracellular proteins.

The results of the current study demonstrate that missense mutations of both the extracellular and intracellular regions of BMPR1A lead to impaired localization of the protein from the cytoplasm to the cell membrane. Previous studies suggest that one potential mechanism is that the mutant proteins are entangled in the ER. Determining the intracellular mediators responsible for these observations is beyond the scope of the current experiments, but further studies should focus on whether there are molecules that bind to mutant BMPR1A proteins and impede them within the cytoplasm, if mutant BMPR1A proteins do not bind as effectively to chaperones responsible for translocation to the cell membrane, or whether endocytosis is increased for mutant receptors.

Acknowledgments

This study was supported by NIH Grants R01CA136884-02 and T32 CA148062-01.

REFERENCES

[1] Burt RW, Bishop DT, Lynch HT, Rozen P, Winawer SJ. Risk and surveillance of individuals with heritable factors for colorectal cancer. Bull WHO 1993;68:655.
[2] Brosens LA, van Hattem A, Hylind LM, et al. Risk of colorectal cancer in juvenile polyposis. Gut 2007;56:965.
[3] Howe JR, Roth S, Ringold JC, et al. Mutations in the SMAD4/DPC4 gene in juvenile polyposis. Science 1998;280:1086.
[4] Howe JR, Bair JL, Sayed MG, et al. Germline mutations of the gene encoding bone morphogenetic protein receptor 1A in juvenile polyposis. Nat Genet 2001;28:184.
[5] Calva-Cerqueira D, Chinnathambi S, Pechman B, Bair J, Larsen-Haidle J, Howe JR. The rate of germline mutations and large deletions of SMAD4 and BMPR1A in juvenile polyposis. Clin Genet 2009;75:79.
[6] Massague J. TGFβ signaling: receptors, transducers, and Mad proteins. Cell 1996;85:947.
[7] Miller SA, Dykes DD, Polesky HF. A simple salting out procedure for extracting DNA from nucleated cells. Nucleic Acids Res 1988;16:1215.
[8] Korchynskyi O, ten Dijke P. Identification and functional characterization of distinct critically important bone morphogenetic protein-specific response elements in the Id1 promoter. J Biol Chem 2002;277:4883.
[9] Chang X, Wang K. wANNOVAR: annotating genetic variants for personal genomes via the web. J Med Genet 2012;49:433.
[10] Ng PC, Henikoff S. Predicting deleterious amino acid substitutions. Genome Res 2001;11:863.
[11] Chun S, Fay JC. Identification of deleterious mutations within three human genomes. Genome Res 2009;19:1553.
[12] Henikoff S, Henikoff JG. Amino acid substitution matrices from protein blocks. Proc Natl Acad Sci U S A 1992;89:10915.
[13] Adzhubei IA, Schmidt S, Peshkin L, et al. A method and server for predicting damaging missense mutations. Nat Methods 2010;7:248.
[14] Schwarz JM, Rodelsperger C, Schuelke M, Seelow D. MutationTaster evaluates disease-causing potential of sequence alterations. Nat Methods 2010;7:575.
[15] Davydov EV, Goode DL, Sirota M, Cooper GM, Sidow A, Batzoglou S. Identifying a high fraction of the human genome to be under selective constraint using GERP++. PLoS Comput Biol 2010;6:e1001025.
[16] Siepel A, Haussler D. Combining phylogenetic and hidden Markov models in biosequence analysis. J Comput Biol 2004;11:413.
[17] Bazykin GA, Kochetov AV. Alternative translation start sites are conserved in eukaryotic genomes. Nucleic Acids Res 2011;39:567.
[18] Allendorph GP, Vale WW, Choe S. Structure of the ternary signaling complex of a TGF-beta superfamily member. Proc Natl Acad Sci U S A 2006;103:7643.
[19] Kotzsch A, Nickel J, Seher A, et al. Structure analysis of bone morphogenetic protein-2 type I receptor complexes reveals a mechanism of receptor inactivation in juvenile polyposis syndrome. J Biol Chem 2008;283:5876.
[20] Rudarakanchana N, Flanagan JA, Chen H, et al. Functional analysis of bone morphogenetic protein type II receptor mutations underlying primary pulmonary hypertension. Hum Mol Genet 2002;11:1517.
[21] Sobolewski A, Rudarakanchana N, Upton PD, et al. Failure of bone morphogenetic protein receptor trafficking in pulmonary arterial hypertension: potential for rescue. Hum Mol Genet 2008;17:3180.
[22] Nishanian TG, Waldman T. Interaction of the BMPR-IA tumor suppressor with a developmentally relevant splicing factor. Biochem Biophys Res Commun 2004;323:91.
[23] Watanabe H, Shionyu M, Kimura T, Kimata K, Watanabe H. Splicing factor 3b subunit 4 binds BMPR-IA and inhibits osteochondral cell differentiation. J Biol Chem 2007;282:20728.